J Mater Sci: Mater Electron (2017) 28:3509–3514
DOI 10.1007/s10854-016-5950-y

Influence of Be substitution on the superconducting properties of $(Cu_{0.5}Tl_{0.5})Ba_2(Ca_{2-y}Be_y)(Cu_{2.5}Cd_{0.5})O_{10-\delta}$ (y = 0, 0.1, 0.2, 0.35, 0.5) samples

M. Rahim[1] · Najmul Hassan[1] · Nawazish A. Khan[2]

Received: 25 August 2016 / Accepted: 24 October 2016 / Published online: 1 November 2016

Abstract Be doped $(Cu_{0.5}Tl_{0.5})Ba_2(Ca_{2-y}Be_y)(Cu_{2.5}Cd_{0.5})O_{10-\delta}$ (y = 0, 0.1, 0.2, 0.35, 0.5) superconductive samples are synthesized by solid state reaction method at normal pressure. The X-ray diffraction of these samples reveals a suppression in the *c*-axis length with the enhanced Be contents, reflecting the incorporation of Be at the inter plane Ca sites. The critical temperature T_c (R = 0) and onset temperature of diamagnetism T_c (onset) are found to increase with the increasing Be-contents up to y = 0.2 and decrease beyond this doping level. The room temperature resistivity, $\rho_{(290K)}$, is decreased in y = 0.1 and 0.2 samples, and raised to higher values beyond y = 0.2 in comparison to y = 0 samples. This improvement most likely arises due to the better interplane coupling caused by incorporation of Be at the Ca sites in the unit cell. The magnitude of diamagnetism is suppressed in all the Be-doped samples in comparison to un-doped sample. The FTIR absorption spectra show systematic hardening of the vibrational modes of apical oxygen with the increasing Be concentration. It confirms the incorporation of Be at the interplane Ca sites which results in the enhanced interplane coupling and hence the better superconducting properties in y = 0.1 and 0.2 samples. This hardening of the apical oxygen modes also complements our XRD results. The suppression of superconductivity parameters in samples with higher Be contents, namely y = 0.35 and 0.5, is attributed to the presence of heavier Cd at the Cu planar sites in CuO_2/CdO_2 planes. Cd atoms suppress the phonon's population due to anharmonic oscillations it produces. Such anharmonicity is further promoted due to the enhanced interplane coupling caused by Be doping which further suppresses the phonon's density and hence the superconductivity in the samples with higher Be-contents i.e. y = 0.35 and 0.5. These results stress on the vital role the electron–phonon interactions in the mechanism of superconductivity in cuprate superconductors.

✉ M. Rahim
m_rahim81@yahoo.com

[1] Department of Physics, Hazara University, Mansehra, Pakistan

[2] Materials Science Laboratory, Department of Physics, Quaid-i-Azam University, Islamabad 45320, Pakistan

1 Introduction

In order to explore the mechanism of superconductivity in oxide high T_c cuprate superconductors, the scientific community has always stressed on the unit cell of these materials [1–4]. The general unit cell of these high temperature superconductors (HTSC) contains two main parts i.e. the charge reservoir block and the superconducting block. These two blocks are separated by Ba atoms. The charge reservoir block, $(Cu_{0.5}Tl_{0.5})Ba_2O_{4-\delta}$, in CuTl-based cuprates is semi-conducting. The superconducting block contains CuO_2 planes separated by Ca atoms and these planes ultimately determine the critical temperature and mechanism of superconductivity in HTSC [5, 6]. Conductivity along these planes is higher than the conductivity along the *c*-axis direction which results in large anisotropy (ξ_{ab}/ξ_c).

Among the cuprate HTSC, $(Cu_{0.5}Tl_{0.5})Ba_2Ca_{n-1}Cu_{n+4-\delta}$ superconductors are most promising due their low penetration depth, relatively low toxicity compared to $TlBa_2Ca_{n-1}Cu_{n+4-\delta}$, normal pressure synthesis and semi-conducting charge reservoir layer $(Cu_{0.5}Tl_{0.5})Ba_2O_{4-\delta}$ [7, 8]. The T_c (R = 0) is optimum for the *n* = *3* member of this family [9–11]. However the anisotropy of this

compound is greater than its parent compound, $CuBa_2Ca_{n-1}Cu_{n+4-\delta}$. So in order to have small values of anisotropy and enhanced interplane coupling, it is often preferred to replace the larger sized Ca^{2+} ions (ionic radius = 0.99 Å) by smaller sized and more electronegative ions like Mg^{2+} (0.65 Å) and Be^{2+} (0.45 Å) [12–19].

Cd had been doped in the CuO_2 planes at Cu site in $(Cu_{0.5}Tl_{0.5})Ba_2Ca_{n-1}(Cu_{n-y}Cd_y)O_{2n+4-\delta}$ (n = 3,4) superconductors [20, 21]. The idea behind those studies was the investigation of any possible role of electron–phonon interactions in the mechanism of high T_c superconductivity i.e. when Cu (a lighter atom) is replaced by Cd (heavier atom), due to the huge difference in mass, the phonons associated with Cd would be different than those associated with Cu. Thus the doping of Cd would give rise to anharmonic oscillations which in turn results in the suppression of density of the desired phonons required for optimum superconductivity. The lack of optimum phonon's population was expected to reduce density of the Cooper pairs. As the Fermi vector (K_F) depends on the number density of the carriers so it would also be reduced. Such a decrease in K_F would suppress the coherence length [$\xi_c = \hbar^2 K_F/\pi m\Delta$] as well as the Fermi velocity (V_F) of the carries and thus the superconductivity [10, 22–24]. The conclusion of the above studies was that the role of electron–phonon interaction is pivotal for superconductivity in HTSC. In the present work, we have doped Be at the Ca interplane sites in $(Cu_{0.5}Tl_{0.5})Ba_2(Ca_{2-y}Be_y)(Cu_{2.5}Cd_{0.5})O_{10-\delta}$ superconductive samples for further elaboration of the above conclusions. The distance between the CuO_2 planes and hence the *c*-axis length, are expected to be decreased with the enhanced incorporation of Be in the unit cell. When the planes will come closer together, the interplane coupling will be improved. But in spite of the better interplane coupling, it is expected that the anharmonicity of Cd atoms will become more pronounced.

2 Experimental

Be-doped $(Cu_{0.5}Tl_{0.5})Ba_2(Ca_{2-y}Be_y)(Cu_{2.5}Cd_{0.5})O_{10-\delta}$ (y = 0, 0.1, 0.2, 0.35, 0.5) superconductive samples were synthesized by well known solid state reaction technique at normal pressure in two steps. The precursor material, $Cu_{0.5}Ba_2(Ca_{2-y}Be_y)(Cu_{2.5}Cd_{0.5})O_{10-\delta}$, was prepared in first step by mixing $Ca(NO_3)_2$, $Ba(NO_3)_2$, $Cd(NO_3)_2$, BeO and Cu(CN) compounds according to the formula unit and grinding for an hour in a quartz mortar and pestle. This ground material was then fired twice at 860 °C in a quartz boat for 24 h followed by furnace cooling to room temperature. In the 2nd step, the fired precursor was ground for an hour and was mixed with a calculated amount of Tl_2O_3 (according to the formula unit) to yield $(Cu_{0.5}Tl_{0.5})Ba_2(Ca_{2-y}Be_y)(Cu_{2.5}Cd_{0.5})O_{10-\delta}$ superconductors as final compounds. The Tl_2O_3 mixed materials were pelletized at 4 tons/cm^2 pressure and the pellets were enclosed in gold capsule. The pellets containing capsule was heat treated in a pre-heated furnace (860 °C) for 10 min. The samples were then quenched to room temperature.

The dc-electrical resistivity measurements of the synthesized samples were carried out with the four probe technique, keeping the current across the sample constant i.e. 1 mA. These measurements were performed during the heating cycle by varying the temperature between 77 and 290 K and rectangular shape samples of dimensions 4.5 mm × 2 mm × 8 mm were used. The ac-susceptibility was measured by using mutual inductance method. For determination of the crystal structure and phase purity, XRD of the samples was carried out by using fine powder X-ray diffraction method. We used the D8 Fuscous diffractometer from BRUKER with Cu-Kα source having wavelength of 1.54056 Å. The data of X-ray diffraction scans was then analyzed with the chekcell refinement software [25].

For Fourier transform infrared (FTIR) absorption spectra we used the NICOLET 5700 spectrometer and recorded the spectra in the wave number range from 400 to 700 cm^{-1}. KBr was used as background material with 200 scans while 500 scans of the spectra were recorded for each sample to minimize the signal to noise ratio.

3 Results and discussion

The X-ray diffraction scans of $(Cu_{0.5}Tl_{0.5})Ba_2(Ca_{2-y}Be_y)(Cu_{2.5}Cd_{0.5})O_{10-\delta}$ (y = 0, 0.1, 0.2, 0.35, 0.5) superconductive samples are shown in Fig. 1a, b. These scans reveal the crystal structure of the samples to be orthorhombic with PMMM space group. All the samples show predominantly single phase nature i.e. (Cu-Tl)-1223 phase. The unit cell parameters determined from the XRD data are as follows. The *a*-axis length is found to be 4.335, 4.330, 4.330, 4.320 and 4.340 Å while the *b*-axis length is 4.125, 4.200, 4.200, 4.120 and 4.200 Å for y = 0, 0.1, 0.2, 0.35 and 0.5, respectively. The *c*-axis length is 14.200, 14.280, 14.145, 14.100, 14.000 Å for the increasing order of Be-content (y), respectively. The *a* and *b*-axes lengths are marginally altered, Fig. 1d, whereas the *c*-axis length is decreased with the increasing Be doping, Fig. 1c. The suppression in the *c*-axis length most likely arises due to the incorporation of Be at the Ca interplane sites. As ionic radius of Be^{2+} (0.45 Å) is smaller than that of Ca^{2+} (0.99 Å) so incorporation of the Be cause to decrease the separation between the CuO_2/CdO_2 planes and hence suppresses the *c*-axis length [26].

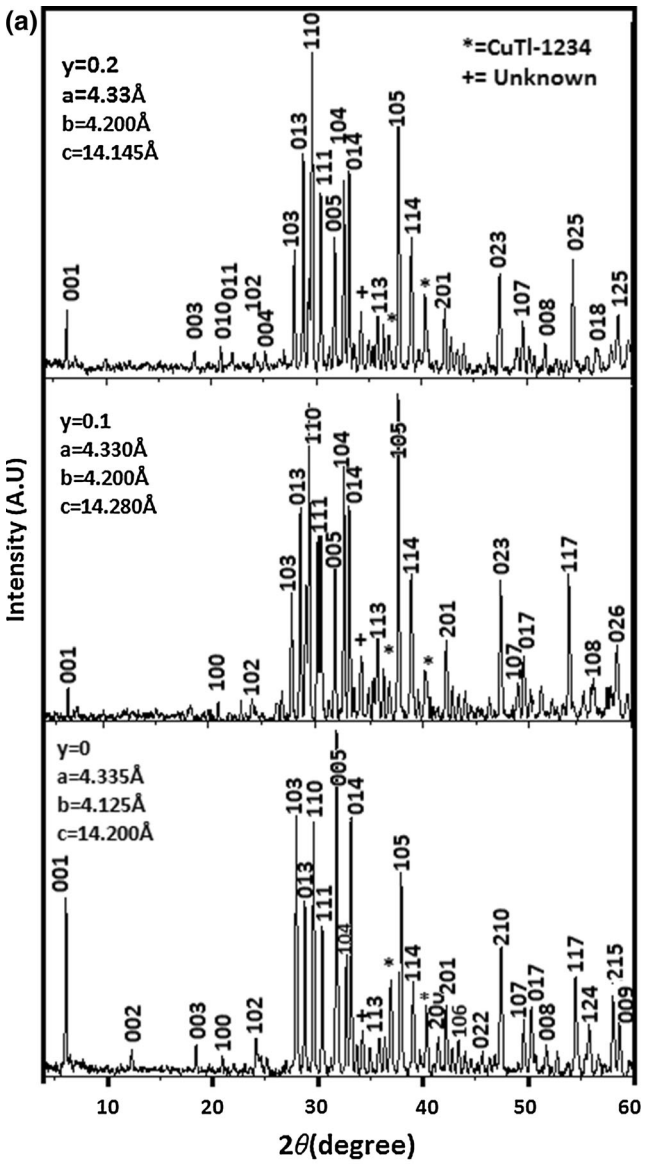
(a)
y=0.2
a=4.33Å
b=4.200Å
c=14.145Å
*=CuTl-1234
+= Unknown
y=0.1
a=4.330Å
b=4.200Å
c=14.280Å
y=0
a=4.335Å
b=4.125Å
c=14.200Å
Intensity (A.U)
2θ(degree)

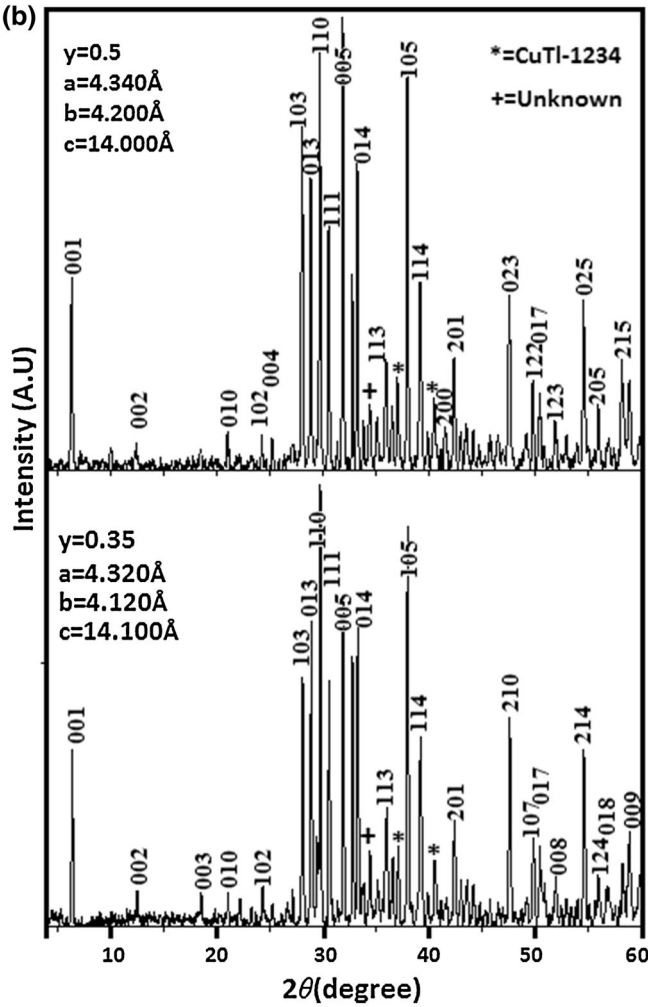
(b)
y=0.5
a=4.340Å
b=4.200Å
c=14.000Å
*=CuTl-1234
+=Unknown
y=0.35
a=4.320Å
b=4.120Å
c=14.100Å
Intensity (A.U)
2θ(degree)

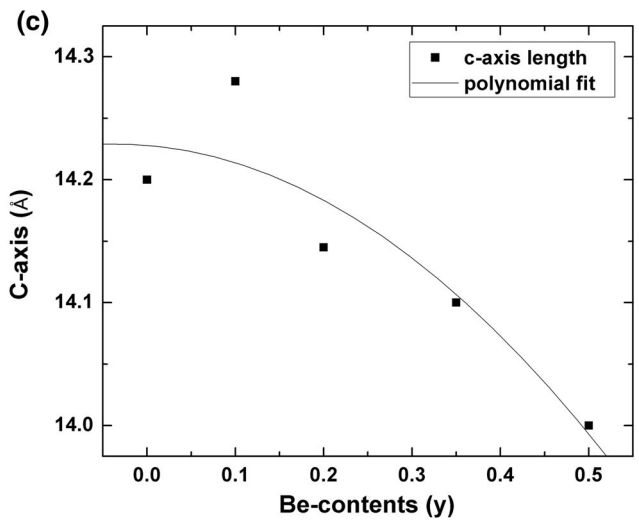
(c)
c-axis length
polynomial fit
C-axis (Å)
Be-contents (y)

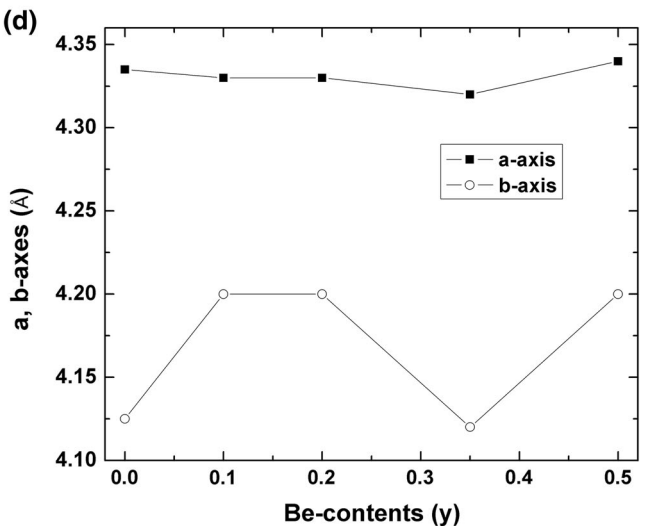
(d)
a-axis
b-axis
a, b-axes (Å)
Be-contents (y)

◀**Fig. 1** **a** XRD scans of $(Cu_{0.5}Tl_{0.5})Ba_2(Ca_{2-y}Be_y)(Cu_{2.5}Cd_{0.5})O_{10-\delta}$ (y = 0, 0.1, 0.2) superconductors. **b** XRD scans of $(Cu_{0.5}Tl_{0.5})Ba_2(Ca_{2-y}Be_y)(Cu_{2.5}Cd_{0.5})O_{10-\delta}$ (y = 0.35, 0.5) superconductors. **c** Plot of c-axis length versus Be-content (y) for $(Cu_{0.5}Tl_{0.5})Ba_2(Ca_{2-y}Be_y)(Cu_{2.5}Cd_{0.5})O_{10-\delta}$ (y = 0, 0.1, 0.2, 0.35, 0.5) superconductors. **d** Plot of a and b-axis lengths versus Be-content (y) for $(Cu_{0.5}Tl_{0.5})Ba_2(Ca_{2-y}Be_y)(Cu_{2.5}Cd_{0.5})O_{10-\delta}$ (y = 0, 0.1, 0.2, 0.35, 0.5) superconductors

Variation in dc-electrical resistivity with temperature for these samples is shown in Fig. 2a. The resistivity of all the samples varies in a metallic way up to onset of superconductivity as the temperature is lowered. T_c (R = 0) for Be free sample (y = 0) is observed around 100 K whereas it is increased to 107 and 108 K for the samples with Be contents of y = 0.1 and 0.2, respectively. For further increase in the doping level of Be, the T_c (R = 0) is decreased to 102 and 93 K in the samples with y = 0.35 and 0.5, respectively; see Fig. 2b. $\rho_{(290K)}$, in $(Cu_{0.5}Tl_{0.5})Ba_2(Ca_{2-y}Be_y)(Cu_{2.5}Cd_{0.5})O_{10-\delta}$ (y = 0, 0.1, 0.2, 0.35, 0.5) samples is found to be 0.206, 0.122, 0.181, 0.310 and 0.410 Ω-cm for the increasing order of y, respectively. This data shows that T_c (R = 0) is increased and the $\rho_{(290K)}$ is decreased with the enhanced Be-concentration up to y = 0.2 while the T_c (R = 0) is suppressed and the $\rho_{(290K)}$ is enhanced for further increase in Be contents, namely y = 0.35 and 0.5, as compared to un-doped (y = 0) samples. The suppression in normal state resistivity and increase in T_c (R = 0) are attributed to the better interplane coupling brought about by the incorporation of smaller sized Be^{2+} ions at the larger sized Ca^{2+} ions [5]. On the other hand, the suppression of T_c (R = 0) and enhancement in the normal state resistivity most likely arise due to the presence of heavier Cd ions in the CuO_2 planes that induce anharmonic oscillations. This anharmonicity is further increased when the planes come closer together due to Be-doping pointing to the fact that the electron–phonon interactions are somehow involved in the mechanism of superconductivity in these materials [20, 26].

The ac-susceptibility versus temperature graphs for our samples are displayed in Fig. 3a, b. All the samples reflect diamagnetic behavior below T_c (onset) in the in-phase component of susceptibility (χ'). Values of T_c (onset), from the χ' plots are found to be 101, 106, 108, 103 and 93 K for y = 0, 0.1, 0.2, 0.35 and 0.5 respectively. From the out of phase component (χ''), the peak temperature (T_p) is observed at 96, 103, 105 and 99 K for y = 0, 0.1, 0.2 and 0.35 samples, respectively; whereas the y = 0.5 sample has not shown any peak. The magnitude of diamagnetism ($|\chi'|_{(77K)}$) is suppressed in all the Be-doped samples as compared to y = 0 sample.

Although the mechanism of superconductivity in HTSC is unknown but still role of the electron–phonon interactions cannot be excluded [27]. The phonon modes related to different oxygen atoms in the unit cell of cuprate superconductors are of immense importance. Such oxygen vibrational modes in Tl-based high T_c cuprates lie above 300 cm^{-1} wave number [28–32]. These vibrational modes in the unit cell are categorized as (1) the apical oxygen modes (2) the planar oxygen modes and (3) the O_δ oxygen modes. As the charge reservoir layer of CuTl-based superconductors contains Cu as well as Tl atoms so the apical oxygen modes are of two types, namely Cu(1)–O_A–Cu(2) and Cu(1)–O_A–Tl. These apical modes are observed around 420–480 and 540 cm^{-1} while the planar and O_δ oxygen modes are found around 580 and 692 cm^{-1} respectively [28, 30].

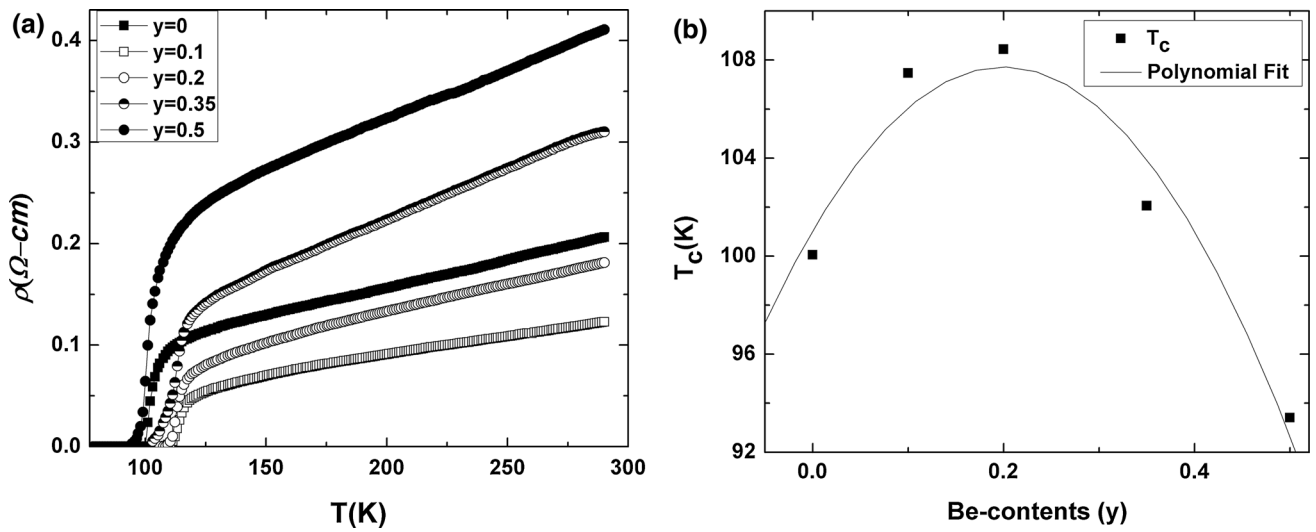

Fig. 2 **a** DC-electrical resistivity versus temperature graphs of $(Cu_{0.5}Tl_{0.5})Ba_2(Ca_{2-y}Be_y)(Cu_{2.5}Cd_{0.5})O_{10-\delta}$ (y = 0, 0.1, 0.2, 0.35, 0.5) samples. **b** T_c (R = 0) versus Be-contents plot for $(Cu_{0.5}Tl_{0.5})Ba_2(Ca_{2-y}Be_y)(Cu_{2.5}Cd_{0.5})O_{10-\delta}$ (y = 0, 0.1, 0.2, 0.35, 0.5) samples

Plots of the FTIR absorption spectra for $(Cu_{0.5}Tl_{0.5})Ba_2(Ca_{2-y}Be_y)(Cu_{2.5}Cd_{0.5})O_{10-\delta}$ (y = 0, 0.1, 0.2, 0.35, 0.5) samples are depicted in Fig. 4. The apical oxygen mode of type Cu(2)/Cd–O_A–Tl have two branches i.e. Cd–O_A–Tl and Cu(2)–O_A–Tl. The earlier is observed about 420 cm^{-1} in all the samples while the later is found around 438, 444, 457, 457 and 457 cm^{-1} for the ascending order of y. The other apical oxygen mode of type Cu(2)/Cd–O_A–Cu(1) is also branched into two due the presence of Cd; the vibrational modes of type Cd–O_A–Cu(1) are observed around 479, 485, 492, 503 and 485 cm^{-1} for y = 0, 0.1, 0.2, 0.35 and 0.5 samples, respectively, while the modes of type Cu(2)–O_A–Cu(1) are found around 539, 536, 535, 536 and 534 cm^{-1} for the ascending order of Be-contents (y). This data shows that the apical oxygen modes of type Cu(2)–O_A–Tl and Cd–O_A–Cu(1) are systematically hardened with the increasing concentration of Be. The planar oxygen modes of vibration, namely Cu(2)–O_p–Cu(1), are observed about 570, 568, 570, 567 and 570 cm^{-1} for y = 0, 0.1, 0.2, 0.35 and 0.5 samples, respectively. This marginal alteration of the planar modes show that there is no systematic variation in the lengths of *a* and *b*-axes which is in agreement with our XRD results, Fig. 1d. The O_δ oxygen mode almost stays fixed about 692 cm^{-1} in all the samples and its intensity is almost constant indicating that the oxygen contents in our samples are at their optimum level. This data shows systematic hardening of the phonon modes of apical oxygen with the increasing Be concentration. Such hardening implies shortening of the apical oxygen bond length which indicates the incorporation of Be at the Ca interplane sites in the unit cell of our samples. Our XRD results i.e.

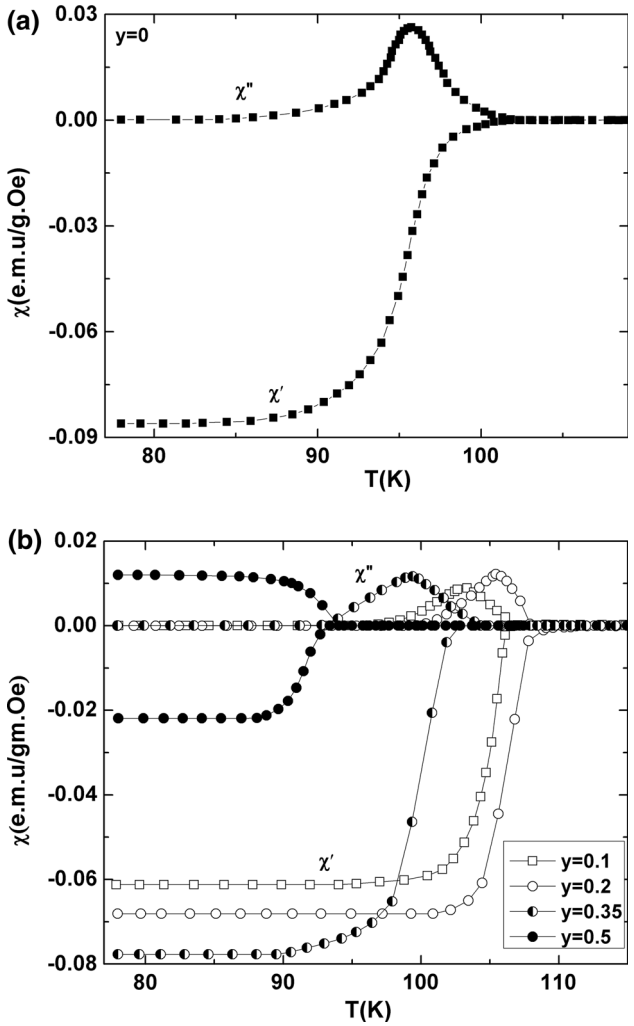

Fig. 3 **a** AC-susceptibility versus temperature plot of $(Cu_{0.5}Tl_{0.5})Ba_2Ca_2(Cu_{2.5}Cd_{0.5})O_{10-\delta}$ superconductive sample. **b** AC-susceptibility versus temperature graphs of $(Cu_{0.5}Tl_{0.5})Ba_2(Ca_{2-y}Be_y)(Cu_{2.5}Cd_{0.5})O_{10-\delta}$ (y = 0.1, 0.2, 0.35, 0.5) samples

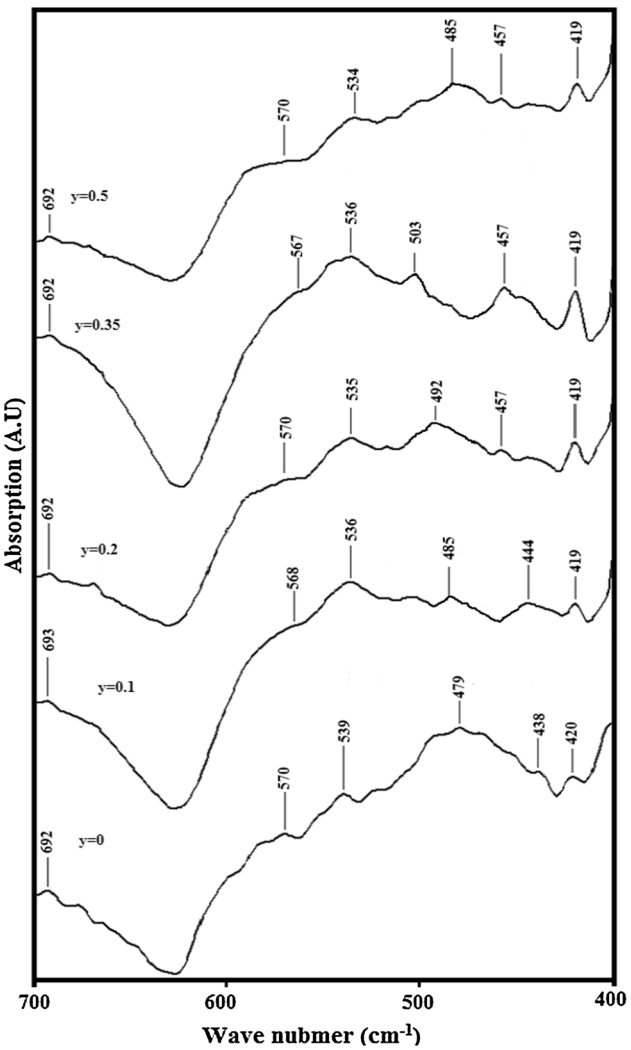

Fig. 4 FTIR absorption spectra of $(Cu_{0.5}Tl_{0.5})Ba_2(Ca_{2-y}Be_y)(Cu_{2.5}Cd_{0.5})O_{10-\delta}$ (y = 0, 0.1, 0.2, 0.35, 0.5) superconductors

suppression of the *c*-axis length is also complemented by the FTIR results i.e. hardening of the phonon modes of apical oxygen.

4 Conclusions

The XRD results of our $(Cu_{0.5}Tl_{0.5})Ba_2(Ca_{2-y}Be_y)(Cu_{2.5}Cd_{0.5})O_{10-\delta}$ (y = 0, 0.1, 0.2, 0.35, 0.5) samples show that length of the *c*-axis of the unit cell is reduced with the enhanced Be-concentration. The suppressed *c*-axis shows that the distance between the CuO_2 planes is decreased with the increasing Be-contents in the unit cell of our samples. T_c (R = 0), from the resistivity measurements is found to increase with the increasing Be-doping up to y = 0.2 i.e. from 100 k (for y = 0) to 108 K (for y = 0.2) and is decreased beyond this doping level. The T_c (onset) and T_p from the susceptibility data also show the same trend as found for T_c (R = 0) with the increasing Be-contents. The improvement in T_c, T_p and T_c (onset) most likely arises due to the better interplane coupling brought about by the incorporation of Be at the Ca sites between the planes. Whereas the suppression of these parameters for higher doping concentrations of Be may be arising due to the presence of heavier Cd atoms in the CuO_2 planes. Influence of the anharmonic oscillations induced by Cd atoms becomes more pronounced when the planes come closer together thereby suppressing the population of the desired phonons required for optimum superconductivity. The FTIR results of our samples show systematic hardening of the apical phonon modes of vibration at 438 and 479 cm^{-1} that indicate the decreased bond length of the apical oxygen. Shortening of the apical oxygen bond length implies suppression of the *c*-axis length and thus the FTIR results of our samples agree with the XRD results. These studies emphasize on the fact that the electron–phonon interactions play a fundamental role in the mechanism of superconductivity in cuprate superconductors.

Acknowledgements Higher Education Commission of Pakistan (HEC) is highly acknowledged for providing the financial support for this work through Project No. 21-623/SRGP/R&D/HEC/2015.

References

1. H. Zhang, H. Sato, Phys. Rev. Lett. **70**, 1697 (1993)
2. T.H. Geballe, Science **259**, 1550 (1993)
3. J. Orenstein, A.J. Millis, Science **288**, 468 (2000)
4. M. Karppinen, H. Yamauchi, Y. Morita, M. Kitabatake, T. Motosahi, R.S. Liu, J.M. Lee, J.M. Chen, J. Solid State Chem. **177**, 1037 (2004)
5. N.A. Khan, S.A. Manzoor, J. Appl. Phys. **105**, 113923 (2009)
6. C. Park, R.L. Synder, J. Am. Ceram. Soc. **78**, 3171 (1995)
7. Hideo Ihara, Kazuyasu Tokiwa, Hirotomo Ozawa, Masayuki Hirabayashi, Akira Negishi, Hirofumi Matuhata, Young Seok Song, Jpn. J. Appl. Phys. **33**, L503–L506 (1994)
8. M.H. Julien, P. Carretta, M. Horvactic, C. Berthier, Y. Berthier, P. Segransan, A. Carrington, D. Calson, Phys. Rev. Lett. **76**, 4238 (1996)
9. J. Akimoto, K. Tokiwa, A. Iyo, H. Ihara, H. Hayakawa, Y. Gotoh, Y. Osawa, Phys. C **279**, 181 (1997)
10. H. Ihara, A. Iyo, K. Tanaka, K. Tokiwa, K. Ishida, N. Terada, M. Tokumoto, Y. Sakita, T. Tsukamoto, T. Watanabe, M. Umeda, Phys. C **282–287**, 1973 (1997)
11. H. Ihara, in *Advances in Superconductivity VII*, vol. 1, ed. by K. Yamafuji, T. Morishita (Springer, Tokyo, 1995), p. 255
12. S.K. Agarwal, A. Iyo, K. Tokiwa, Y. Tanaka, K. Tanaka, M. Tokumoto, N. Terada, T. Saya, M. Umeda, H. Ihara, Phys. Rev. B **58**, 9504 (1998)
13. N.A. Khan, A.A. Khurram, Appl. Phys. Lett. **86**, 152502 (2005)
14. N.A. Khan, A. Javed, A.A. Khurram, Phys. C **425**, 90 (2005)
15. A.A. Khurram, N.A. Khan, Supercond. Sci. Technol. **19**, 679 (2006)
16. N.A. Khan, Shahid Nawaz, IEEE Trans. Appl. Supercond. **16**, 2 (2006)
17. N.A. Khan, G. Hasnain, K. Sabeeh, J. Phys. Chem. Solids **67**, 1841 (2006)
18. N.A. Khan, G. Husnain, Phys. C **436**, 51 (2006)
19. M. Mumtaz, A. Nawazish, J. Khan, Appl. Phys. **103**, 083913 (2008)
20. N.A. Khan, M. Rahim, J. Alloys Compd. **481**, 81 (2009)
21. Nawazish A. Khan, Asad Raza, J. Supercond. Nov. Magn. **23**, 199 (2010)
22. J. Bardeen, L.N. Cooper, J.R. Schrieffer, Phys. Rev. **108**, 1175 (1957)
23. Michael Tinkham, *Introduction to Superconductivity*, 2nd edn. (McGraw-Hill Inc, New York, 1996), p. 125
24. H. Ihara, A. Iyo, K. Tanaka, K. Tokiwa, N. Terada, M. Tokumoto, K. Ishida, M. Umeda, in *Advances in Superconductivity IX*, vol. 1, ed. by S. Nakajima, M. Murakami (Springer, Tokyo, 1996), p. 277
25. S.O. Al-Asbahi, R.M. Kershi, J. Chem. Crystallogr. **42**, 155 (2012)
26. M. Rahim, N.A. Khan, J. Alloys Compd. **527**, 74 (2013)
27. X.-J. Chen, V.V. Struzhkin, Z. Wu, R.J. Hemely, H. Mao, H.-Q. Lin, Phys. Rev. B **75**, 134504 (2007)
28. W. Kress, U. Schroder, J. Prade, A.D. Kulkarni, F.W. de Welte, Phys. Rev. B **38**, 2906 (1988)
29. A.D. Kulkarni, J. Prade, F.W. de Welte, W. Kress, U. Schroder, Phys. Rev. B **40**, 2642 (1989)
30. J. Prade, A.D. Kulkarni, F.W. de Welte, Phys. Rev. B **39**, 2771 (1989)
31. A.D. Kulkarni, F.W. de Welte, J. Prade, U. Schroder, W. Kress, Phys. Rev. B **41**, 6409 (1990)
32. N.A. Khan, M. Mumtaz, K. Sabeeh, M.I.A. Khan, M. Ahmed, Physica C **407**(3–4), 103 (2004)